

## EARLY-TIME INFRARED SPECTRA OF THE TYPE Ia SUPERNOVA 2000cx

RICHARD J. RUDY,<sup>1</sup> DAVID K. LYNCH,<sup>1</sup> S. MAZUK,<sup>1</sup> CATHERINE C. VENTURINI,<sup>1</sup> R. C. PUETTER,<sup>2</sup> AND P. HÖFLICH<sup>3</sup>

Received 2001 June 15; accepted 2001 September 21

### ABSTRACT

We present 0.8 to 2.5  $\mu\text{m}$  spectra of the Type Ia supernova 2000cx from 8 and 7 days before maximum light. The spectra consist of a continuum that closely follows that of a hot blackbody (25,000 K) upon which is superposed a small number of absorption and emission features. The most prominent absorption is due to the Mg II multiplet at 1.0926  $\mu\text{m}$  (rest frame); the strongest emission feature is at  $\sim 1.25 \mu\text{m}$  and is probably due to Fe III. The broad Si II feature at  $\sim 1.65 \mu\text{m}$ , if present, is very weak. There is no evidence of the He I singlet at 2.0581  $\mu\text{m}$ . Velocities in the Mg II feature extend to beyond 20,000  $\text{km s}^{-1}$ , indicating that carbon burning reached the outermost layers of the progenitor, and providing support for the delayed detonation models. The blackbody shape of the continuum beyond 0.9  $\mu\text{m}$  is used to provide a limit on the in situ reddening of  $E(B-V) \leq 0.1$  mag. Given the probable uniformity of the early-time spectra of Type Ia supernovae (SNe Ia), this technique should be applicable to other SNe Ia. Multicolor light curves reported by other observers indicate that SN 2000cx was over-luminous, suggesting a higher than usual production of  $^{56}\text{Ni}$ . This can account for the hotter than normal continuum and the generally higher excitation of the line features.

*Subject headings:* infrared: stars — supernovae: individual (SN 2000cx)

### 1. INTRODUCTION

Infrared spectra of Type Ia supernovae (SNe Ia) from shortly after outburst can provide information that is difficult or impossible to obtain at any other wavelength or epoch (Höflich 1997; Wheeler et al. 1998). This stems from the nature of both the explosion and of the progenitor itself.

There is general agreement that SNe Ia result from some process of combustion of a degenerate white dwarf (WD) (Hoyle & Fowler 1960) in a binary system. Within this general picture, three classes of models have been considered: (1) An explosion of a carbon oxygen (CO) WD, with mass close to the Chandrasekhar limit. The WD accretes mass through Roche-lobe overflow from an evolved companion star (e.g., Whelan & Iben 1973; Livio 2000). The explosion is triggered by compressional heating near the WD center. (2) An explosion of a rotating configuration formed from the merging of two low-mass WDs, caused by the loss of angular momentum due to gravitational radiation (Webbink 1984; Iben & Tutukov 1984; Paczyński 1985). (3) Explosion of a low mass CO-WD triggered by the detonation of a helium layer (Nomoto 1980; Woosley, Weaver, & Taam 1980; Woosley & Weaver 1986). Only the first two models appear to be viable. The third, the sub-Chandrasekhar WD model, has been ruled out on the basis of predicted light curves and spectra (Höflich & Khokhlov 1996). Of the two remaining models, the first is the most widely favored scenario of SNe Ia. In it, as the WD accretes material from its binary companion, its mass increases and its radius decreases. The energy release due to adiabatic compression and the heat wave from the surface burning is

balanced by cooling processes but, overall, the temperature in the WD rises. The compressibility of the WD increases with mass, as does the surface burning and the temperature. Thermonuclear runaway occurs when the temperature close to the center becomes sufficiently high that the nuclear burning timescales become shorter than the hydrodynamical timescales. This occurs when the mass of the WD is very close to the Chandrasekhar limit. The carbon burning that commences near the WD center then proceeds outward subsonically as a deflagration. Burning in this region reaches statistical equilibrium, producing iron group elements. The outer layers of the star respond to the pressure wave from this burning, which advances at the sound speed, by swelling up and expanding away from the center. In order for the burning front to overtake the receding outer layers (and synthesize the elements that match the observations), the burning front must accelerate. This occurs when the deflagration becomes a detonation or a very fast deflagration. Even so, densities and temperatures in the outer layers are low enough that the nuclear burning is incomplete, that is, burning of silicon does not occur. This results in the production of measurable amounts of intermediate mass elements, chiefly neon, magnesium, silicon, sulfur, and calcium.

These delayed detonation (DD) and deflagration models (Khokhlov 1991; Yamaoka et al. 1992; Woosley & Weaver 1994) have been found to reproduce the optical and infrared light curves and spectra of “typical” SNe Ia reasonably well. As mentioned above, the DD models assume that burning starts as subsonic deflagration and then turns into a supersonic, detonative mode of burning. Due to the one-dimensional nature of the models, the speed of the subsonic deflagration and the moment of the transition to a detonation are free parameters. The moment of the deflagration-to-detonation transition (DDT) is conveniently parameterized by introducing the transition density,  $\rho_{\text{tr}}$ , at which the DDT happens. The amount of  $^{56}\text{Ni}$  depends primarily on  $\rho_{\text{tr}}$  (Höflich 1995; Umeda et al. 1999), and to a lesser extent on the assumed value of the deflagration speed,

<sup>1</sup> Space Science Applications Laboratory, The Aerospace Corporation M2/266, P. O. Box 92957, Los Angeles, CA 90009; richard.j.rudy@aero.org, david.k.lynch@aero.org, stephan.m.mazuk@aero.org, catherine.c.venturini@aero.org.

<sup>2</sup> Center for Astrophysics and Space Sciences, University of California at San Diego C-0111, La Jolla, CA 92093; rpuetter@ucsd.edu.

<sup>3</sup> Department of Astronomy, University of Texas, Austin, TX 32611; pah@hej1.as.utexas.edu.

initial central density of the WD, and initial chemical composition, primarily the ratio of carbon to oxygen. (In fact, Umeda et al. 1999 suggest that  $\rho_{\text{tr}}$  may depend strongly on the C/O ratio but both the size and sign of the effect is still under discussion.) Models with smaller transition densities give less nickel and hence both slightly lower peak luminosities and temperatures. However, because the DDs predict nearly complete burning of the WD, the total production of nuclear energy is almost constant from event to event.

Alternatively, pure deflagration models can also adequately describe many aspects of the supernovae population (Höflich & Khokhlov 1996; Hatano et al. 2000). In particular, the classical “deflagration” model W7 of Nomoto, Thielemann, & Yokoi (1984) has successfully reproduced optical light curves and spectra (e.g., Harkness 1987). The basic difference between the fast deflagration and delayed detonation models is the degree of burning. As noted above, very nearly the entire WD is burned in the DD models. Little unburned carbon remains in the outer layers, having been replaced with the products of explosive carbon burning such as neon and magnesium. These elements have minimum ejection velocities between  $\sim 11,000$  and  $15,000 \text{ km s}^{-1}$  with the bulk of the material reaching significantly greater values (Höflich, Khokhlov, & Wheeler 1995; Höflich, Wheeler, & Thielemann 1998b). In contrast, in the deflagration models no burning takes place at velocities much over  $15,000 \text{ km s}^{-1}$  and neon and magnesium are confined to lower velocities, typically  $11,000$  to  $14,000 \text{ km s}^{-1}$  (Höflich & Khokhlov 1996).

To select between the various models of SNe Ia explosions, spectroscopic observations that probe the velocity and compositional structure of the outer layers of the WD are needed. The importance of early-time observations is that shortly after outburst the outer layers are still dense and compact and imprint a signature upon the spectrum (Khokhlov 1991; Ruiz-LaPunte et al. 1992). The advantage present in the near-infrared is that the principal opacity source at early epochs is electron scattering and is thus independent of wavelength, giving the photosphere a well-defined radius and velocity (Wheeler et al. 1998). This is not true at visible and ultraviolet wavelengths where strong resonance transitions dominate the opacity. Unfortunately, early-time infrared spectra of SNe Ia events are scarce due to the relatively recent advent of both systematic supernova searches and the widespread use of infrared spectrographs. SN 2000cx, a relatively bright Type Ia supernova, was discovered 2000 July 17.5 (UT) by Yu, Modjaz, & Li (2000). We were at Lick Observatory shortly after discovery and obtained near-infrared spectra on two consecutive nights that turned out to be 8 and 7 days prior to visible maximum. In this paper we present and discuss these data.

## 2. OBSERVATIONS

The infrared spectrophotometric data were acquired on the nights of 2000 July 20 and 21 (UT) with the 3 m Shane reflector of Lick Observatory. The instrument used was the Aerospace Near-Infrared Imaging Spectrograph (NIRIS), which is described in more detail by Rudy, Puetter, & Mazuk (1999). Briefly, the spectrograph uses two channels, each containing a collimator, grating, camera, and detector array, to provide nearly continuous coverage between  $0.8$  and  $2.5 \mu\text{m}$ . A beam splitter that switches from reflection to transmission at  $1.38 \mu\text{m}$  separates the channels. The detec-

tors employed were two-quadrant NICMOS3 devices providing 256 channels in the spectral dimension and 128 in the spatial. The spatial resolution is  $1''$  per pixel. A  $600 \text{ line mm}^{-1}$  grating blazed at  $1.0 \mu\text{m}$  operates in the “blue” channel, while a  $300 \text{ line mm}^{-1}$  blazed at  $2.0 \mu\text{m}$  services the red. Each channel has a nearly constant resolution,  $16 \text{ \AA}$  for the blue channel and  $37 \text{ \AA}$  for the red, with the  $3''$  slit width used for the observations of SN 2000cx.

To remove the instrumental response and reduce the effects of atmospheric absorption, the raw spectra of SN 2000cx were reduced by dividing by the spectrum of the comparison star HD 191854. HD 191854 is a solar analog with  $V = 7.45$ . To remove its intrinsic spectrum from this ratio, a solar model from Kurucz (1991) was used. An absolute flux scale was set by normalizing to the  $K$  magnitude for HD 191854 of 5.95. The  $K$  magnitude was calculated from the  $V$  magnitude tabulated in the Bright Star Catalog (Hoffleit & Jaschek 1982) and the nominal  $V - K$  color for a G5 dwarf from Koorneef (1983). With the exception of the wavelengths regions around Mg II  $\lambda 10926$ , the spectra from the two nights were very similar. They were combined to produce the spectrum shown in Figure 1; the Mg II data are plotted for each of the nights in Figure 3.

## 3. RESULTS

SN 2000cx was located on the outskirts of the S0 galaxy NGC 524 in a region free from dust and star formation Chornock et al. (2000). Both Chornock et al. (2000) and Krisciunas (2001) reported that SN 2000cx was overluminous. The light curves indicate that SN 2000cx reached its maximum in the  $V$  band on Julian Date  $2451754.0 \pm 0.3$  (W. D. Li 2001, private communication), reaching a magnitude of 13.25, very similar to the value in the  $B$  band reported by Leonard et al. (2000). Taking a heliocentric velocity for NGC 524 of  $+2421 \text{ km s}^{-1}$ , correcting this for infall into the Virgo cluster ( $270 \text{ km s}^{-1}$ ), and employing a value of  $63 \text{ km s}^{-1} \text{ Mpc}^{-1}$  for the Hubble constant, gives  $M_V = -19.42$ . The Galactic reddening in the direction of NGC 524 is thought to be  $E(B - V) \sim 0.08$  (Schlegel, Finkbeiner, & Davis 1999), which implies  $M_V$  was more like  $-19.7$  and definitely greater than the nominal value of  $-19.34 \pm 0.17$  (Jha et al. 1999). A higher than normal peak luminosity for SN 2000cx was also indicated by the slower decline rate. The  $\Delta m_{15}$  value, which is the decline in the  $B$  magnitude in the 15 days following maximum light (Phillips 1993), of  $0.98 \pm 0.05 \text{ mag}$  is definitely smaller than the nominal value of 1.10 (Leibundgut 1988) and is consistent with the greater absolute brightness.

The following discussion focuses on three features that appear in the early-time near-infrared spectrum of SN 2000cx: the blackbody nature of the continuum, the Mg II absorption feature at approximately  $1.0 \mu\text{m}$ , and the Fe III emission at  $1.25 \mu\text{m}$ . All three can be seen in Figure 1 and are discussed in separate sections below. Additional features that are present or notably absent from the spectrum are discussed in a fourth subsection. We begin with the near-infrared continuum and show how it can be utilized to estimate the reddening.

### 3.1. The Near-Infrared Continuum and the Reddening

The blackbody nature of the early-time infrared continuum is reflected in the models of SNe Ia spectra. It is a consequence of electron scattering, which is the dominant

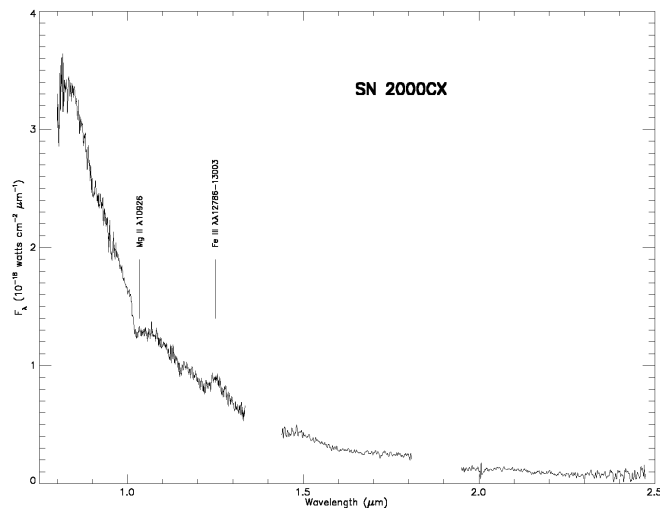


FIG. 1.—Near-infrared spectrum of SN 2000cx from 2000 July 20 and 21. The spectrum is the average of the two nights of data. The Mg II  $\lambda 10926$  absorption is the feature centered at  $1.03 \mu\text{m}$  and is due to three transitions:  $\lambda 10914$ ,  $\lambda 10915$ , and  $\lambda 10952$ . The emission bump at  $1.25 \mu\text{m}$  is produced primarily by transitions of Fe III (see text). The Si II emission feature at  $1.65 \mu\text{m}$  seen in other Type Ia events is very weak if present at all.

opacity source (Wheeler et al. 1998). While not a true continuum generating process, electron scattering provides the necessary path length to enhance the effects of the free-free, free-bound, and bound-bound opacities. Note that this is not the case in the ultraviolet and optical portions of the spectrum where strong atomic transitions dominate the opacity. Moreover, these conditions do not persist for long. Shortly after maximum light, expansion thins the material, after which atomic transitions determine the opacity in the infrared as well. By about 7 days after  $M_V$ , the well-known “J band” absorption (Elias et al. 1981, 1985; Frogel et al. 1987; Lynch et al. 1992) appears. This is actually a deficit of flux due to the absence of opacity sources (Höflich, Khokhov, & Muller 1993; Spyromilio, Pinto, & Eastman 1994) or, more precisely, a region of low line blending bracketed by regions with high line opacities due to iron group elements (Wheeler et al. 1998).

The degree to which the continuum of SN 2000cx follows a hot blackbody is apparent in Figure 2. The smooth, solid line represents a 25,000 K blackbody, corrected for the Galactic reddening of  $E(B-V) = 0.083$ , whose level is adjusted to match that of the supernova at  $2.1 \mu\text{m}$ . This temperature represents a best-fit value—there is a substantial departure from a pure Rayleigh-Jeans spectrum and, likewise, a 10,000 K blackbody is a noticeably poorer fit. Significant differences between the spectrum and the blackbody occur at only a few points, the most notable being that of the Mg II feature (discussed in the following section), and at wavelengths less than  $0.9 \mu\text{m}$ , where other absorption features become manifest. The temperature is significantly greater than any derived from the fits Meikle et al. (1996) made to the continuum of SN 1994D. This is in large measure due to the fact that they included the optical portion of the spectrum, fitting to the envelope defined by the regions relatively free of absorption features. Because of the large electron scattering opacity (Harkness 1987 predicts an optical depth of  $\sim 50$  at the time of our

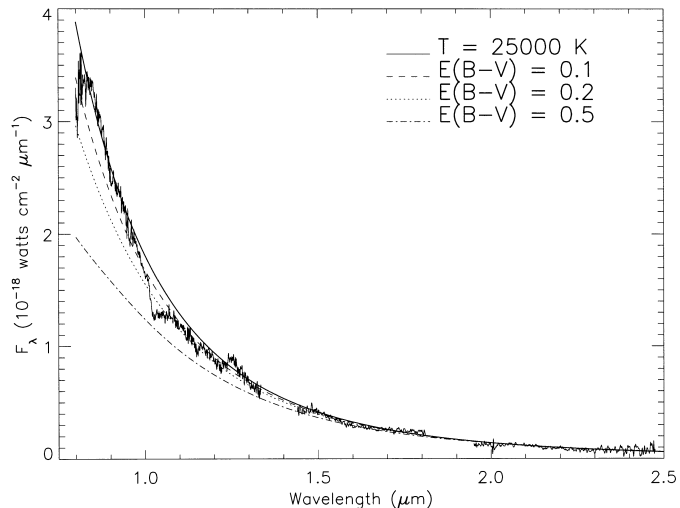


FIG. 2.—Blackbody fit to the near-infrared continuum of SN 2000cx and the effects of extinction. The fit is a 25,000 K blackbody corrected for the Galactic extinction of  $E(B-V) = 0.083$  and scaled to the observations. The other curves show the effects of various additional amounts of extinction (potentially representing extinction occurring local to SN 2000cx or in its parent galaxy) on the blackbody. All curves are normalized to match the observations at  $2.1 \mu\text{m}$ . Even small amounts of extinction produce measurable departures from the observations, so it is likely that then in situ extinction is less than 0.1 in  $E(B-V)$ .

observations) the infrared continuum forms at deeper, and thus hotter, layers.

However, the temperature of SN 2000cx may actually be hotter than that of SN 1994D due to a slightly greater amount of  $^{56}\text{Ni}$  that was synthesized. In the following section data are presented that indicate nuclear burning in SN 2000cx reached far out into the stellar envelope. In particular, the region of explosive carbon burning extended to very high velocities. We note that this is consistent with a higher  $^{56}\text{Ni}$  production expected from models (see below).

As noted earlier, the Galactic reddening in the direction of SN 2000cx, as estimated by the *COBE/IRAS* results (Schlegel et al. 1998) is  $E(B-V) = 0.083$ . Some extinction along the line of sight to SN 2000cx is also indicated by the mean  $B-V$  color of 0.18 in the period leading up to maximum light. The blackbody shape of the early-time infrared spectrum can be utilized to estimate the total extinction. This is illustrated in Figure 2. The effects of three different reddening values on the 25,000 K blackbody, in addition to the nominal Galactic value, are shown. The reddened values are again normalized to the observations at  $2.1 \mu\text{m}$  and the reddening curve of Draine (1990) is employed. What can be seen is that large extinction values [e.g.,  $E(B-V) = 0.5 \text{ mag}$ ] produce sizeable departures from the observations, and that even small values (0.1 mag) are distinguishable.

Limits on the in situ reddening, depend, of course, upon the true color temperature of the infrared continuum of SN 2000cx and the actual value of the Galactic reddening, parameters that are not entirely separable from our observations. If the value of  $E(B-V) = 0.083$  for the reddening due to the Galaxy is correct, and the infrared continuum was pure Rayleigh-Jeans ( $F_\lambda \sim \lambda^{-4}$ , requiring  $T > 10^5$ ), the local reddening could be as large as  $E(B-V) = 0.15$  although the temperature seems unrealistically high and the fit is not as good as that shown in Figure 2. Conversely, if

there is no extinction at all, a temperature of 20,000 K produces a good match to the observations, but a significantly smaller value ( $T = 15,000$  K) does not. Thus, our observations indicate that the intrinsic color temperature of the infrared continuum is between 20,000 and 25,000 K and that the total extinction is probably less than 0.2. As pointed out by Chornock et al. (2000), SN 2000cx lies on the outskirts of a S0 galaxy in a region that is apparently free of dust so its local reddening is expected to be small. Our results suggest that this in situ reddening is less than 0.1, and possibly zero.

Before leaving this topic it seems worthwhile to point out that if the uniformity of SNe Ia spectra extends to the infrared, as is indicated by the models, the shape of the infrared continuum could provide a general method for estimating the extinction. Given that the dispersion in Type Ia luminosities, after correction for decline rate, is 0.14 mag in the  $V$  band (Hamy et al. 1996), and that 0.25 mag has significant implications for a cosmological constant (Filippenko & Riess 2000), an accurate assessment of the extinction is critical for each Type Ia supernova. Employing the shape of the near-infrared continuum to derive the extinction, which requires only a single measurement, may provide an important addition to those methods that use fits to the multi-color light curves (e.g., Lira et al. 1998; Krisciunas et al. 2000).

### 3.2. The Mg II $\lambda 10926$ Feature

The strongest absorption feature in the early-time infrared spectrum of SN 2000cx is Mg II  $\lambda 10926$ . It was seen in the early-time spectra of SN 1994D by Meikle et al. (1996) and was conclusively identified by Wheeler et al. (1998) with three transitions ( $\lambda 10914$ ,  $\lambda 10915$ ,  $\lambda 10952$ ) that occur between the  $4^2P^o$  and  $3^2D$  terms of singly ionized magnesium. Magnesium is produced by the burning of carbon in Type Ia supernovae. It is formed throughout the WD but persists only in regions where temperatures and densities are low enough that burning does not proceed to heavier elements. As such, it is produced and survives only in the outermost layers that undergo significant nuclear processing. Because of this, the magnesium spectral features display some of the highest outflow velocities of any of the elements synthesized in the supernova explosion. Moreover, the inner boundary of the magnesium region delineates the region where carbon burning ends and oxygen burning, which gives rise to the intermediate mass elements such as silicon, sulfur, and calcium, begins. This underscores its diagnostic importance. However, because it forms in the fastest moving material, and thus the material that is first to dissipate, it is short lived, hence the importance of early-time spectra. The specific utility of the Mg II  $\lambda 10926$  absorption is due both to the spectral region in which it resides and to the intermediate strength of the atomic transitions that produce it. Although there are stronger features of Mg II present in the UV and optical portions of the spectrum, these are either blended with additional features or are so strong that trace amounts of magnesium that existed prior to the explosion produce measurable, and confusing, additional features. For example, the well-known Mg II UV feature at  $\sim 2800$  Å is extremely strong. In SNe Ia, it forms somewhere in the outer layers even at late times when the photosphere has receded far into the central layers. Thus, it does not locate the velocity at which the transition from explosive carbon burning to explosive oxygen burning

occurs, a parameter that can distinguish between deflagration and delayed detonation models (Dominguez, Höflich, & Straniero 2001). In contrast, the weaker (but still strong) Mg II  $\lambda 10926$  transition is surrounded by a well-formed continuum and is produced in strength only in the large amounts of material freshly synthesized in the explosion.

In Figure 3, the Mg II absorption is plotted as a function of velocity space for the two nights of the observations. In both cases the steep continuum has been removed by subtracting a linear fit to the data on both sides of the Mg II feature. There are two aspects of the absorption features that we wish to point out. First, a comparison of the two nights suggests that the deepest part of the feature shifted slightly toward longer wavelengths. A similar shift was observed in SN 1994D between 8.5 and 5.5 days prior to maximum light (Meikle et al. 1996). However, the velocity shift observed in SN 2000cx appears to be less than the 2000 to 3000 km s<sup>-1</sup> per day change expected from a variety of explosion models (e.g., Höflich & Khokhlov 1996) in which the shift is due to the recession of the photosphere through the velocity region in which the feature is formed. Moreover, the appearance of the Fe III features at  $\sim 1.25$   $\mu$ m (see § 3.3 below) indicates that the photosphere was already within this velocity range at the time of our observations. This suggests that subtle shift in the deepest part of the absorption feature was probably due to small changes in the excitation and opacity of the absorbing material.

The second point is that, although we cannot exactly identify the velocity at which the transition from carbon to oxygen burning occurred, it was not very much smaller than the 20,000 km s<sup>-1</sup> value marked by the deepest point of the absorption feature seven days before maximum light. Such a large value is in direct conflict with the deflagration models, as is the extreme blue wing of the feature which extends to nearly 25,000 km s<sup>-1</sup> from line center. (Note that this is only the observed velocity extreme—significant amounts of undetected material might be present at higher

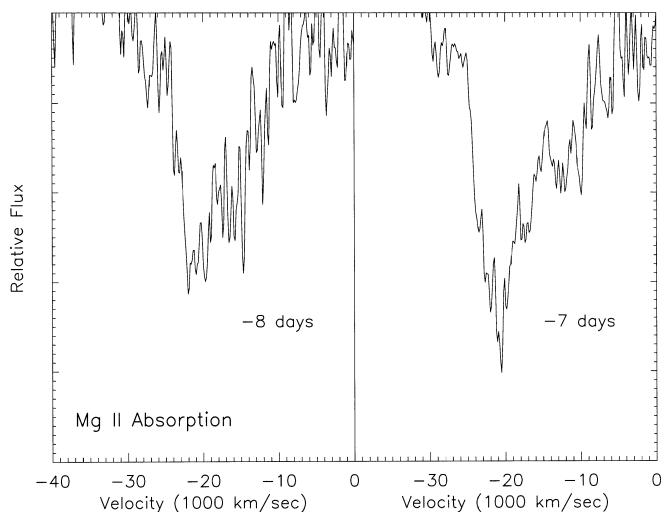


FIG. 3.—Mg II  $\lambda 10926$  feature from 8 and 7 days before  $V$  maximum [2000 July 20 and 21 (UT), respectively]. Note that the feature is deeper on the second night and that velocity of minimum flux is at a slightly smaller velocity. The blue edge of the feature extends to  $\sim 25,000$  km s<sup>-1</sup> on both nights, indicating that explosive carbon burning extended quite far out in the expanding envelope.

velocities.) These velocities are significantly greater than the  $15,000 \text{ km s}^{-1}$  maximum predicted by the W7 model of Nomoto et al. (1984) and require delayed detonation models such as DD21 of Höflich (1997), or DD200 of Höflich, Wheeler, & Khokhlov (1998a). The detonation allows the nuclear flame to overtake the rapidly expanding outer layers, extending element synthesis to greater velocities.

It is worthwhile noting that mixing within the expanding layers cannot reconcile the extreme velocities observed for the Mg II feature in SN 2000cx with the much lower velocities predicted by the pure deflagration models. State of the art three-dimensional models of the deflagration phase (e.g., Khokhlov 2002) show Ni and Si plumes rising up to a region encompassing about 0.5 to 0.7 the mass of the star. At this time, however, the overall pre-expansion results in a freezing out of the structure (after about 2 s), and no similar mixing of the Mg layer takes place. Even if the plumes could rise further, they would carry the products of explosive oxygen burning (i.e., products of complete or incomplete Si burning). In contrast, magnesium clearly results from explosive carbon burning. Some mixing of Mg to lower velocities is not ruled out, but this only enhances the disparity between the deflagration models and the observations of SN 2000cx.

Returning again to a comparison with SN 1994D, the Mg II feature in that object did not extend to the extreme wavelengths observed in SN 2000cx (Meikle et al. 1996). Compared to SN 1994D, the nuclear burning in SN 2000cx extended further out and the region of explosive carbon burning was shifted toward higher velocities. These properties, like the greater temperature of its continuum and its probable overluminosity, are consistent with a higher production of  $^{56}\text{Ni}$ .

### 3.3. Fe III at $1.25 \mu\text{m}$

The most prominent “emission” feature in the spectrum is the bump at  $1.25 \mu\text{m}$  with the possible P Cygni wing (see Fig. 1). This feature has not been discussed previously in the literature and was not modeled for this study, but a review of the models generated to understand the spectrum of SN 1994D (Höflich 1995) suggests that this feature is probably due to three strong transitions of Fe III:  $^7S_3-^7P_4$   $\lambda 12786$ ,  $^7S_3-^7P_3$   $\lambda 12920.56$ ,  $^7S_3-^7P_2$   $\lambda 13003.39$ , with possible contributions from several, weaker transitions of Ni III. Unfortunately, the early-time measurements of SN 1994D of Meikle et al. (1996), which extended to 8.5 days before maximum, did not include this portion of the spectrum. The synthetic spectra of Wheeler et al. (1998) did include this wavelength region but did not consider spectra earlier than 3 days before maximum light. We believe that the three Fe III transitions are the probable sources of the feature since the higher than normal excitation manifested by SN 2000cx could make  $\text{Fe}^{+2}$ , rather than  $\text{Fe}^+$ , the dominant ionization state of iron at the epoch of our measurements. Additional evidence for a higher than normal excitation was provided by Chornock et al. (2000), who reported the presence of strong Fe III absorption features in the optical spectrum 5 days before maximum light but noted that the lower excitation Si II  $\lambda 6120$  (the signature feature of SNe Ia) was weak. The laboratory wavelengths for the features together with the values observed in SN 2000cx indicate an expansion velocity of  $12,000\text{--}13,000 \text{ km s}^{-1}$  for this material, and that the photosphere had receded to

this point at the time of our observations. This is consistent with models (Höflich et al. 1998a, 1998b) which also indicate the presence of freshly synthesized Fe at these velocities.

### 3.4. Other Features

There are a few additional spectral features that are notable for either their presence or absence in the data. The Si II “emission” at  $\sim 1.65 \mu\text{m}$  is one of the former and is discussed by Wheeler et al. (1998). It is weaker in SN 2000cx than in SN 1994D, a fact we once again attribute to the slightly higher excitation of the former.

The synthetic spectra of Wheeler et al. (1998) from 3 days before  $V$  maximum show a feature at  $\sim 1.12 \mu\text{m}$  that is due to Ca II  $\lambda 11839$  and  $\lambda 11950$ , two strong transitions from comparatively low energy levels. Their absence in SN 2000cx is understandable due to the earlier time of the spectra; the excitation of the spectrum is still too high to support these features. The Ca II feature was also missing from the early time spectrum of SN 1994D.

Finally, there is no evidence of the He I single  $\lambda 20581$  in the spectrum SN 2000cx. Helium is not expected to be evident in the spectrum and its presence in detectable quantities would be contrary to the explosion of a white dwarf at the Chandrasekhar limit.

## 4. SUMMARY AND CONCLUSION

Near-infrared spectra of SN 2000cx from 8 and 7 nights before  $V$  maximum show a continuum that matches closely that of a  $25,000 \text{ K}$  blackbody. The most distinctive spectral features are the absorption due to Mg II  $\lambda 10926$  and an emission bump at  $1.25 \mu\text{m}$  that we suggest is due primarily to Fe III. The velocity of the Mg II feature extends well beyond  $20,000 \text{ km s}^{-1}$  and indicates that carbon burning in SN 2000cx reached very high velocities. This lends support to the so-called delayed detonation models in which a deflagration front eventually becomes a detonation; it argues strongly against pure deflagration models. From the delayed detonation models, we expect that the amount of  $^{56}\text{Ni}$  and the maximum velocity for explosive oxygen burning would increase together (Höflich 1995). The near-infrared spectrum of SN 2000cx, and the spectral differences between SN 2000cx and SN 1994D, are in accord with these expectations. The excitation level of the spectrum, as reflected in both the temperature indicated by the continuum and in the spectral features present, appears higher than normal and is commensurate with SN 2000cx having been an overluminous event.

Finally, the comparison between the near-infrared continuum and a blackbody that was used to measure the reddening in SN 2000cx should provide an additional means for measuring the extinction in other SNe Ia since the infrared continua of all these objects are expected to be similar.

We thank K. Baker and W. Earthman, the telescope operators at Lick Observatory during these measurements, and T. Armstrong, for their help in acquiring the data. We are grateful to W. D. Li for providing light curves of SN 2000cx, and to K. Krisciunas who also provided results from photometric monitoring. An anonymous referee provided a number of very helpful and detailed comments. C.

Rice also provided several helpful comments. This work was supported by The Aerospace Corporation's Independent Research and Development program and by the US Air Force Space and Missile Systems Center through the Mission Oriented Investigation and Experimentation

program, under contract F4701-00-C-0009. R. C. P. acknowledges support from NASA, as does P. H. who was supported in part by NASA grant LSTA-98-022, and by the John W. Cox Endowment Fund to the Department of Astronomy at the University of Texas.

## REFERENCES

- Chornock, R., Leonard, D. C., Filippenko, A. V., Li, W. D., Gates, E. L., & Chloros, K. 2000, *IAU Circ.* 7463
- Draine, B. T. 1990, in *Proc. 22d Esab Symp. on Infrared Spectroscopy in Astronomy (ESA SP-290)* ed. B. H. Kaldeich (Paris: ESA), 93
- Dominguez, I., Höflich, P., & Straniero, O. 2001, *ApJ*, 557, 279
- Elias, J. H., Frogel, J. A., Hackwell, J. A., & Persson, S. E. 1981, *ApJ*, 251, L13
- Elias, J. H., Matthews, K., Neugebauer, G., & Persson, S. E. 1985, *ApJ*, 296, L379
- Filippenko, A. V., & Riess, A. G. 2000, in *Type Ia Supernovae: Theory and Cosmology*, ed. J. C. Niemeyer & J. W. Truran (Cambridge: Cambridge Univ. Press), 1
- Frogel, J. A., et al. 1987, *ApJ*, 315, L129
- Hamy, M., Phillips, M. M., Schommer, R. A., Suntzeff, N. B., Maza, J., & Avilés, R. 1996, *AJ*, 112, 2391
- Harkness, R. 1987, in *13th Texas Symp. on Relativistic Astrophysics* (Singapore: World Scientific), 413
- Hatano, K., Branch, D., Lentz, E. J., Baron, E., Filippenko, A. V., & Garnavich, P. 2000, *ApJ*, 543L, 49
- Höflich, P. 1995, *ApJ*, 443, 89
- . 1997, in *Supernovae and Cosmology*, ed. Labhardt et al., (Binningen: Univ. Basel), 25
- Höflich, P., & Khokhlov, A. 1996, *ApJ*, 457, 500
- Höflich, P., Khokhlov, A., & Müller, E. 1993, *A&A*, 270, 223
- Höflich, P., Khokhlov, A., & Wheeler, J. C. 1995, *ApJ*, 444, 831
- Höflich, P., Wheeler, J. C., & Khokhlov, A. 1998a, *ApJ*, 492, 228
- Höflich, P., Wheeler, J. C., & Thielemann, F. K. 1998b, *ApJ*, 495, 617
- Hoffleit, D., & Jaschek, C. 1982, *The Bright Star Catalog* (New Haven: Yale Univ. Obs.)
- Hoyle, P., & Fowler, W. A. 1960, *ApJ*, 132, 565
- Iben, I. J., & Tutukov, A. V. 1984, *ApJS*, 54, 335
- Jha, S., et al. 1999, *ApJS*, 125, 73
- Khokhlov, A. M. 1991, *A&A*, 245, 114
- . 2002, *ApJ*, in press
- Koornneef, J. 1983, *A&A*, 128, 84
- Krisciunas, K. 2001, *PASP*, 113, 121
- Krisciunas, K., Hastings, N. C., Loomis, K., McMillan, R., Rest, A., Riess, A. G., & Stubbs, C. 2000, *ApJ*, 539, 658
- Kurucz, R. L. 1991, *Precision Astronomy and Astrophysics of the Galaxy*, ed. A. G. Davis Philip, A. R. Uggren, & K. A. Janes (Schenectady: Davis), 1
- Leibundgut, B. 1988, Ph.D. thesis, Univ. Basel
- Leonard, D. C., Filippenko, A. V., Chornock, R., & Li, W. D. 2000, *IAU Circ.* 7471
- Lira, P., et al. 1998, *AJ*, 115, 234
- Livio, M. 2000, in *Type Ia Supernovae: Theory and Cosmology*, ed. J. C. Niemeyer & J. W. Truran (Cambridge: Cambridge Univ. Press), 33
- Lynch, D. K., Erwin, P., Rudy, R. J., Rossano, G. S., Puetter, R. C. 1992, *AJ*, 104, 1156
- Meikle, W. P. S., et al. 1996, *MNRAS*, 281, 263
- Nomoto, K. 1980, *ApJ*, 248, 798
- Nomoto, K., Thielemann, F.-K., & Yokoi, K. 1984, *ApJ*, 286, 644
- Paczynski, B. 1985, in *Cataclysmic Variables and Low-Mass X-Ray Binaries*, ed. D. Q. Lamb & J. Patterson (Dordrecht: Reidel), 1
- Phillips, M. M. 1993, *ApJ*, 413, L108
- Rudy, R. J., Puetter, R. C., & Mazuk, S. 1999, *AJ*, 118, 666
- Ruiz-LaPuntes et al. 1992, *ApJ*, 387, L33
- Schlegel, D. J., Finkbeiner, D. P., & Davis, M. 1998, *ApJ*, 500, 525
- Spyromilio, J., Pinto, P. A., & Eastman, R. G. 1994, *MNRAS*, 266, 17P
- Umeda, H., Nomoto, K., Yamaoka, H., & Wanajo, S. 1999, *ApJ*, 513, 861
- Webbink, R. F. 1984, *ApJ*, 277, 355
- Wheeler, C., Höflich, P., Harkness, R. P., & Spyromilio, J. 1998, *ApJ*, 496, 908
- Whelan, J., Iben, I. Jr. 1973, *ApJ*, 186, 1007
- Woosley, S. E., & Weaver, T. A. 1986, *ARA&A*, 24, 205
- . 1994, *ApJ*, 423, 371
- Woosley, S. E., Weaver, T. A., & Taam, R. E. 1980, in *Type Ia Supernovae*, ed. J. C. Wheeler (Austin: Univ. Texas Press), 96
- Yamaoka, H., Nomoto, K., Shigeyama, T., & Thielemann F. 1992, *ApJ*, 393, 55
- Yu, C., Modjaz, M., & Li, W. D. 2000, *IAU Circ.* 7458